JOURNAL

OF THE AMERICAN CHEMICAL SOCIETY

VOLUME 108, NUMBER 12 JUNE 11, 1986

Carbon CP-MASS NMR and X-ray Crystal Structure of Paramagnetic Lanthanide Acetates

S. Ganapathy,[†] V. P. Chacko,[‡] R. G. Bryant,*[†] and M. C. Etter[§]

Contribution from the Departments of Radiology, Biophysics, and Chemistry, University of Rochester, Rochester, New York 14642, Department of Radiology, Johns Hopkins Medical Center, Baltimore, Maryland 21025, and Department of Chemistry, University of Minnesota, Minneapolis, Minnesota 55455. *Received September 27, 1985*

Abstract: The X-ray crystal structures of praseodymium(III) acetate monohydrate and europium(III) acetate trihydrate have been solved and cross-polarization carbon-13 NMR spectra obtained in the polycrystalline solids. The static and magic angle spinning spectra are compared with diamagnetic acetate spectra. The shifts in the paramagnetic compounds are large, permitting sample heterogeniety to be readily detected. The CP-MASS carbon spectra are assigned by using both relaxation times and dipolar interactions as a guide.

We have recently studied a series of metal acetates by NMR and X-ray crystallographic techniques.[1-4] Diamagnetic metal acetates have been investigated by carbon-13 NMR and the principal elements of the chemical shielding tensor determined.[1] Complete assignments of carbon resonances belonging to chemically similar but magnetically nonequivalent acetate carbons were made in cadmium acetate dihydrate by a detailed single crystal study.[2] Combined application of carbon-13 cross polarization magic angle sample spinning (CP-MASS) NMR and X-ray crystallography has permitted the solid-state transformations taking place in a chemically unstable lead acetate trihydrate to be monitored.[3]

Paramagnetic lanthanide acetates are of interest because the magnetic effects of the rapidly relaxing electrons provide opportunities for spectral selection, analogous to shift reagents in the liquid. Recently we reported that high resolution carbon-13 NMR spectra in the solid could be obtained from selected lanthanide acetates.[4] Although the residual line broadening after magic angle sample spinning was typically 10 ppm, the paramagnetically induced isotropic shifts in the carbon spectra were 350 ppm or greater, giving a spectral resolution of 35 or more, which is adequate for structural applications.

Effects of paramagnetic centers in the solid differ from those in liquids in fundamental ways. In a solution of a paramagnetic shift reagent, the paramagnetic center diffuses rapidly among molecules of interest and usually yields a chemical shift that is appropriate to the rapid chemical exchange average limit; thus, the magnitude of the shift may be controlled by the concentration of the paramagnetic species. In the solid state, however, the paramagnetic nuclei are fixed in the crystal lattice eliminating multisite exchange averaging processes. In addition, the paramagnetic shift has considerable inherent anisotropy. Thus the resultant shift is a function of crystal orientation in the magnetic field. In a polycrystalline sample the resulting powder pattern is broadened by a very large chemical shielding anisotropy (500–1000 ppm for carboxyl carbons). Magic angle sample spinning averages the inhomogeneous parts of the interaction yielding reasonable resolution in the solid. However, the large paramagnetic shielding anisotropy causes many spinning side bands when rotor frequencies are moderate, 2–4 kHz. The separation of center bands from spinning side bands is accomplished easily by using different rotor speeds, though side band suppression techniques should also be helpful.[5,6]

A difficulty with interpretation of solid-state spectra is that assignment of resonances to carbon atoms in the molecule cannot be made based on the normal benchmark assignment strategies used in solution because the paramagnetically induced isotropic chemical shifts in the CP-MASS spectra are large and may be further altered by intermolecular interactions in the crystalline solid, which are absent in solution. In an effort to analyze and assign the observed carbon resonances in the CP-MASS spectra of lanthanide acetates and to understand the origin of the observed shifts and line widths, we have determined the three dimensional crystal structure of praseodymium and europium acetates. The complete assignment of the carbon spectra was accomplished by exploiting differential effects of the paramagnetically induced

[†] Present Address: Professor Robert G. Bryant, Department of Radiology, Box 648, University of Rochester Medical Center, 601 Elmwood Avenue, Rochester, NY 14642.
[†] University of Rochester.
[‡] Johns Hopkins Medical Center.
[§] University of Minnesota.

(1) Ganapathy, S.; Chacko, V. P.; Bryant, R. G. *J. Magn. Reson.* **1984**, *57*, 239–247.
(2) Ganapathy, S.; Chacko, V. P.; Bryant, R. G. *J. Chem. Phys.* **1984**, *81*, 661–668.
(3) Bryant, R. G.; Chacko, V. P.; Etter, M. C. *Inorg. Chem.* **1984**, *23*, 3580–3584.
(4) Chacko, V. P.; Ganapathy, S.; Bryant, R. G. *J. Am. Chem. Soc.* **1983**, *105*, 5491–5492.
(5) Dixon, W. T. *J. Magn. Reson.* **1981**, *44*, 220–223.
(6) Dixon, W. T. *J. Chem. Phys.* **1982**, *77*, 1800–1809.

0002-7863/86/1508-3159$01.50/0

Table I. Crystal Data and Structure Solution Parameters for Praseodymium(III) Acetate Monohydrate, I, and Europium(III) Acetate Trihydrate, II

	I	II
mol formula	$Pr_1O_7C_6H_{11}$	$EuO_9C_6H_{15}$
mol wt	337.1	383.1
a (Å)	8.4083 (7)	9.153 (1)
b (Å)	7.968 (1)	15.264 (2)
c (Å)	15.020 (2)	9.092 (2)
β (0)	93.95 (1)	97.05 (1)
v (Å^3)	1003.9	1260.7
space group, Z	$P2_1/c$, 4	$P2_1/c$, 4
density, (g/cm^3)	2.23	2.02
diffrctmtr	Enraf-Nonius Cad-4	Enraf-Nonius Cad-4
scan mode	$\omega/2\theta$	$\omega/2\theta$
radiatn	Mo Kα	Mo Kα
μ (cm^{-1})	48.8	50.1
emprcl absorptn		
correctn appld	yes	yes
θ_{max}	30°	30°
hkl_{max}	11, 11, 21	12, 21, 12
no. unique reflctns measd	2900	3870
no. reflctns obsd.	2188 $I > 3\sigma(I)$	2905 $I > 3\sigma(I)$
$R = [\sum(\|F_o\| - \|F_c\|)]/\sum F_o$	0.030	0.028
$R_w = (\sum(w\|F_o\| - \|F_c\|)/\sum wF_o^2)^{1/2}$ $w = 1/\sigma^2(F_o)$	0.044	0.037
$(\text{shift/error})_{max}$	0.26	0.76
final elctrn dens diff	0.4, e/Å^3	

carbon spin–lattice relaxation, proton–carbon dipolar interactions, and correlating these effects with the observed molecular and crystal structure.

Experimental Section

Praseodymium and europium acetate (Alpha Products, Inc.) were recrystallized several times from water. The hydrates formed in this way were stable for weeks at ambient temperature as judged by the NMR spectra. Carbon-13 NMR spectra were obtained at room temperature (295 K) in the solid state by proton enhanced NMR on a NMR spectrometer, built in this laboratory, operating at 56.4 MHz for protons and 14.19 MHz for carbon. MASS spectra were obtained on a homemade probe incorporating a barrel type spinner (Doty Scientific, S.C.), and spinning speeds up to 5 kHz were used. Hartmann–Hahn matches were established at r.f. field strength of 10 G for protons and 40 G for carbon, but the proton decoupling field was maintained between 50 and 60 kHz. Proton spin-temperature alternation and carbon quadrature phase cycling schemes were employed to minimize spectral distortion. Chemical shifts in the MASS spectra were measured by using an internal standard of hexamethylbenzene mixed with the sample and were then numerically converted to a tetramethylsilane reference. The contact time was chosen to optimize the signal to noise ratio and was not particularly sensitive to changes in the range of 2 ms. Typically 60 000 transients were averaged for static samples, and 35 000 transients were averaged for spinning samples. Exponential multiplication with line-broadening factors of 100 and 25 Hz were used for static and spinning spectra, respectively.

Crystals of praseodymium acetate monohydrate were obtained as pale green plates by recrystallization from water.[17] Crystals of europium acetate trihydrate, also obtained from water, were clear prismatic crystals. Crystal data and structure solution parameters for praseodymium(III) acetate monohydrate, I, and europium(III) acetate trihydrate, II, are given in Table I. Patterson and Fourier methods were used for structure solutions. Some hydrogen atoms were found on electron density difference maps; others were included at theoretically calculated positions and then subsequently refined isotropically. Methyl hydrogen positions were calculated and used in structure factor calculations, but were not further refined. Full-matrix least-squares refinements were used with the anisotropic thermal parameters for all non-hydrogen atoms. Atomic positional parameters are shown in Table II. Tables of thermal parameters, calculated and observed structure factors, and intra- and intermolecular bond lengths and angles are deposited as supplementary material.

Results and Discussion

Carbon-13 spectra obtained from static samples of polycrystalline praseodymium acetate monohydrate, europium acetate trihydrate, and lanthanum acetate are compared in Figure 1. As in the diamagnetic acetates[1] represented by the lanthanum acetate, the carboxyl region is well-separated from the methyl region. For the lanthanum acetate, the singularities from the anisotropic chemical shielding tensor are complicated and obscured by the lanthanum–carbon dipolar broadening particularly obvious at the carboxyl carbon. In the presence of the paramagnetic center, the resolution of these two carbon types is lost because the associated anisotropies are much larger.

Magic angle sample spinning breaks the anisotropy into a side band pattern with each component separated from the next by the rotor frequency. Nevertheless, the patterns from the different resonances overlap seriously requiring several rotor frequencies to deduce center band positions. Four carbon resonances are identified for praseodymium acetate monohydrate and three carbon resonances for europium acetate trihydrate. The strong absorption at −31 ppm Figure 2C and 2D, is much broader (ca. 400 Hz) due to the overlapping resonances in this region. The effects of changing the paramagnetic nucleus to Eu(III) and the

Table II. Positional Parameters with esd's in Parentheses

atom	x	y	z	B (Å^2)
	(a) Eu(III)acetate·3H_2O			
Eu	0.07875 (2)	0.12902 (1)	0.00838 (2)	1.606 (3)
O1a	−0.0440 (4)	0.1310 (2)	0.2393 (3)	2.65 (6)
O2a	−0.0785 (3)	0.0104 (2)	0.1129 (3)	2.34 (6)
C1a	−0.0963 (5)	0.0550 (3)	0.2260 (5)	2.31 (8)
C2a	−0.1810 (7)	0.0176 (4)	0.3411 (6)	4.9 (1)
O1b	0.2563 (4)	0.1937 (2)	0.2079 (4)	2.80 (6)
O2b	0.2663 (4)	0.0515 (2)	0.1766 (4)	3.38 (7)
C1b	0.3081 (5)	0.1209 (3)	0.2484 (6)	2.95 (9)
C2b	0.4165 (9)	0.1134 (5)	0.3862 (9)	5.8 (2)
O1c	−0.0316 (4)	0.1580 (2)	−0.2501 (3)	2.59 (6)
O2c	−0.1821 (4)	0.1593 (2)	−0.0814 (4)	2.77 (6)
C1c	−0.1614 (5)	0.1665 (3)	−0.2154 (5)	2.41 (8)
C2c	−0.2860 (6)	0.1844 (5)	−0.3324 (6)	4.2 (1)
O1w	0.0612 (3)	0.2857 (2)	−0.0016 (3)	2.38 (6)
O2w	0.2841 (4)	0.1570 (2)	−0.1242 (4)	2.79 (6)
O3w	0.5538 (4)	0.0851 (3)	−0.0398 (7)	5.9 (1)
H1	−0.001 (8)	0.307 (5)	0.062 (8)	6*
H2	0.281 (7)	0.197 (5)	−0.174 (7)	6*
H3	0.357 (8)	0.143 (4)	−0.104 (8)	6*
H1a	−0.2145	−0.0404	0.3127	4*
H2a	−0.1233	0.0151	0.4340	4*
H3a	−0.2669	0.0528	0.3491	4*
H1b	0.4457	0.0544	0.4018	4*
H2b	0.5008	0.1486	0.3762	4*
H3b	0.3717	0.1338	0.4692	4*
H1c	−0.3751	0.3103	0.2108	4*
H2c	−0.2948	0.3601	0.0954	4*
H3c	−0.2688	0.2604	0.1199	4*
	(b) Pr(III)acetate·H_2O			
Pr1	0.45110 (3)	0.12403 (3)	0.28508 (1)	
O1	0.3427 (4)	−0.1604 (4)	0.2161 (2)	
O2	0.1776 (4)	0.0509 (5)	0.2191 (3)	
O3	0.6471 (4)	−0.1237 (4)	0.3071 (2)	
O4	0.6557 (5)	0.0573 (5)	0.4172 (2)	
O5	0.3609 (5)	0.3287 (4)	0.3878 (2)	
O6	0.4187 (5)	0.5947 (4)	0.3570 (2)	
O7	0.3259 (5)	−0.0679 (5)	0.3964 (2)	
C1	0.2013 (6)	−0.1020 (6)	0.2070 (3)	
C2	0.0666 (7)	−0.2159 (9)	0.1806 (5)	
C3	0.7142 (6)	−0.0656 (6)	0.3810 (3)	
C4	0.8632 (8)	−0.1477 (7)	0.4209 (4)	
C5	0.3520 (6)	0.4842 (6)	0.4007 (3)	
C6	0.2578 (8)	0.5429 (7)	0.4768 (4)	
H1	0.074 (0)	−0.325 (0)	0.206 (0)	
H2	0.066 (0)	−0.225 (0)	0.116 (0)	
H3	−0.028 (0)	−0.162 (0)	0.195 (0)	
H4	0.885 (0)	−0.122 (0)	0.481 (0)	
H5	0.951 (0)	−0.110 (0)	0.387 (0)	
H6	0.854 (0)	−0.267 (0)	0.413 (0)	
H7	0.319 (0)	0.547 (0)	0.533 (0)	
H8	0.172 (0)	0.465 (0)	0.480 (0)	
H9	0.218 (0)	0.650 (0)	0.461 (0)	
H11	0.346 (9)	−0.049 (10)	0.450 (5)	
H10	0.342 (10)	−0.143 (9)	0.384 (5)	

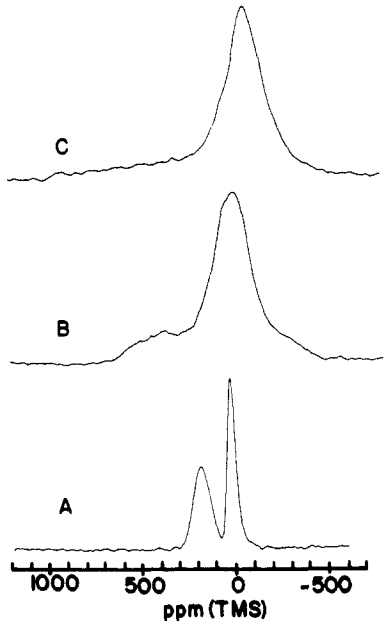

Figure 1. The static proton decoupled carbon-13 cross-polarization NMR spectra of polycrystalline lanthanide acetates obtained at 1.32 T and ambient temperature: (A) lanthanum acetate; (B) praseodymium acetate monohydrate; (C) europium acetate trihydrate.

concomitant changes in solid-state structure are evident in the spectra of freshly recrystallized europium(III) acetate, Figure 2D; two carboxyl resonances of unequal intensity are clearly resolved. Unrecrystallized europium(III) acetate shows additional peaks, Figure 2F, some of which may also be seen in the spectra of samples purposely exposed to an atmosphere of acetic acid Figure 2E. There appear to be two sources of the differences observed: (1) additional water may account for the peak at approximately 300 ppm (Figure 2F) if 30% of the metal atoms have an additional water molecule associated. (2) Storate over acetic acid causes the appearance of several more lines as shown in Figure 2E, some of which appear in the spectrum 2F. These peaks apparently occur in old samples as a result of a slow solid-state hydrolysis reaction. The present observations parallel those reported for lead(II) acetate trihydrate crystals, which readily form multiple solid-state decomposition products.[3] Although the details of the chemical transformations in the solid are not understood, it is clear that sample history is an important parameter to consider when analyzing solid-state NMR spectra.

Praseodymium acetate monohydrate, I, is isostructural with cerium(III) acetate monohydrate[7] but is not isostructural with the trifluoroacetate analogue, Pr(III) $(O_2C_2F_3)_3 \cdot 3H_2O$.[8] In the present investigation it was found that the Pr atom in I is nine coordinate, whereby two acetate groups are bidentate, and one group exists as a bridging group that involves a neighboring Pr in a screw-related molecule. In contradiction to the reported cerium acetate structure,[7] which was solved with limited precision, we find that Pr···O(1) and Pr···O(3) intramolecular bond distances are longer than their intermolecular bonds to Pr atoms in neighboring molecules. The assignment of terms intra and inter is, thus, an arbitrary one for purposes of discussion and is not based on geometrical limits. The ligand coordination and selected bond lengths and angles are shown in Figure 3. An Ortep drawing of the coordination sphere is shown in Figure 4a.

In the unit cell packing pattern of I, Figure 5a, it is seen that the most significant intermolecular interactions are the acetate group bridging screw-related molecules along an extended chain parallel to the *b*-axis and hydrogen bonds which link the two chains in the *c*-direction. The water oxygen O(7) acts as a proton donor

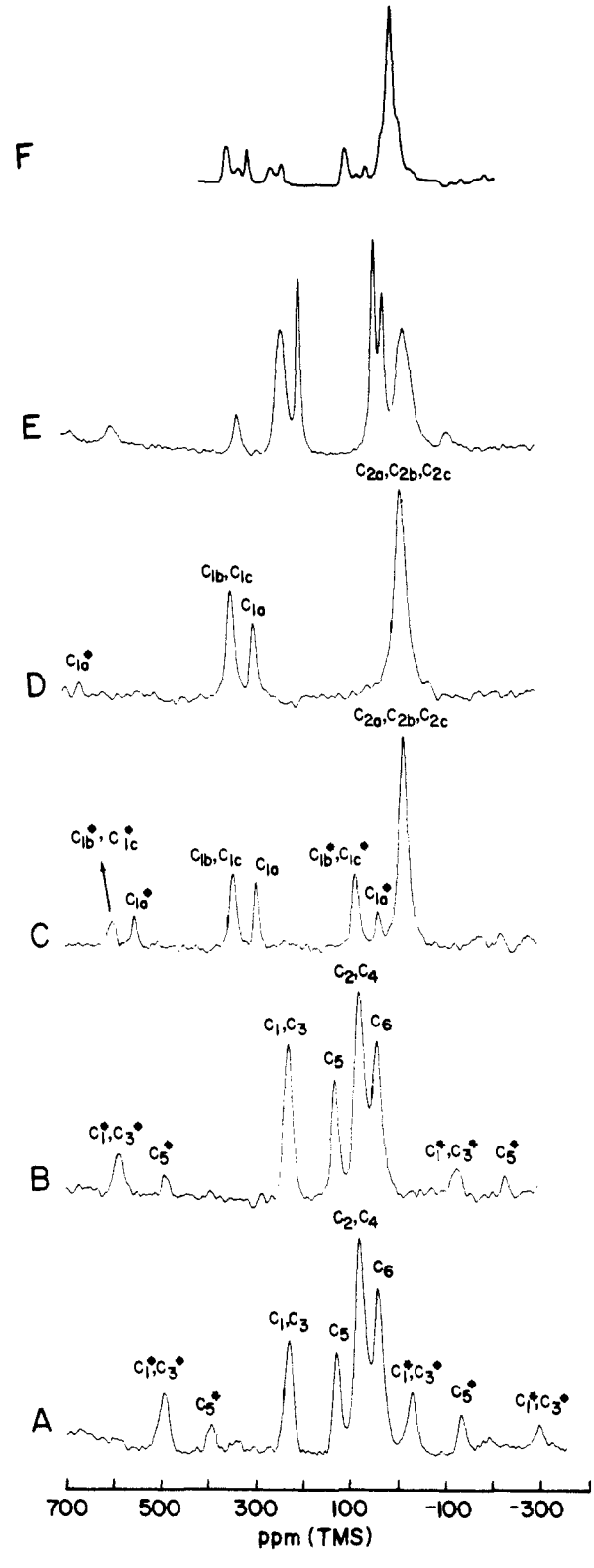

Figure 2. The carbon CP-MASS NMR spectra of paramagnetic lanthanide acetates: (A) praseodymium acetate monohydrate obtained at a rotor frequency of 3.6 kHz; (B) praseodymium acetate monohydrate obtained at a rotor frequency of 5 kHz; (C) europium acetate trihydrate obtained at a rotor frequency of 3.4 kHz; (D) europium acetate trihydrate obtained at rotor frequency of 4.8 kHz; (E) europium acetate after storage over acetic acid for 1 week, obtained, at a rotor frequency of 4.8 kHz; (F) europium acetate xH_2O (AlphSample) obtained at a rotor frequency of 3.3 kHz. The assignments shown correspond to the carbon atoms indicated in the X-ray structure, Figure 4. * corresponds to a spinning side band.

(7) Sadikov, G. G.; Kukina, G. A.; Porai-Koshits, M. A. *Zh. Strukt. Khim.* **1967**, *8*, 551–553.
(8) Bone, S. P.; Sowerby, B. D.; Verma, R. D. *J. Chem. Soc., Dalton Trans.* **1978**, 1544–1548.

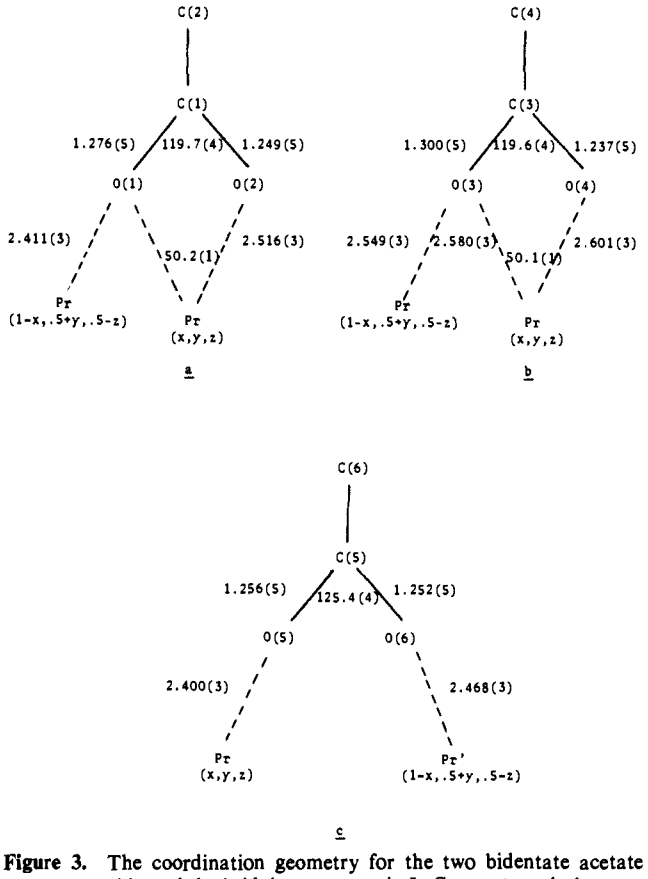

Figure 3. The coordination geometry for the two bidentate acetate groups, a and b, and the bridging group, c, in I. Symmetry relations are indicated. The Pr···O–C–O planes for a–c are planar to within 0.06 Å. The dihedral angle between least-squares planes of Pr···O–C–O in a and b is 39°, between a and c, 73°, and b and c, −74°.

to O(4) on an *i*-related molecule ($1-x, -y, 1-z$) and to O(6) on another *i*-related molecule ($-x, 1-y, -z$). O(7) is also coordinated as an electron donor to Pr.

In europium(III) acetate trihydrate, II, the europium atom is nine coordinate, bonding to two water oxygens and three bidentate acetate groups. The ninth ligand is from O(2) on a neighboring molecule ($-x, -y, -z$), Figure 4b. The coordination geometry and selected bond distances and angles are shown in Figure 6. It may be seen that the intramolecular Eu···O(2) distance is longer than the intermolecule Eu···O(2) distance. The O1–C2–O2 acetate group could be considered a bridging group with a weak secondary bidentate interaction. As for I, hydrogen bonds constitute the predominant intermolecular interactions. O1w and O2w are coordinated directly to Eu, but O3w hydrogen bonds only to other oxygen atoms, shown in Figure 4b, and in the steroscopic Ortep view of the unit cell, Figure 5b. Each Eu–acetate group is essentially planar, as for I. The interplanar angles between these acetates are: 101, 101, and 98 degrees for a–b, a–c, and b–c torsion angles (a, b, c and correspond to the planes of atoms with those subscripts in Figure 4b).

Since the assignment procedures often employed in the carbon-13 MASS spectra may be misleading because of paramagnetic contributions to the shift, carbon relaxation rates were used as the primary guide in these spectra. The carbon resonance relaxation will be dominated by the electron–nuclear dipole–dipole interactions, the correlation time for which we assume to be the electron relaxation times, which are thus the same as sensed by each carbon atom. The relative comparisons of carbon relaxation times will thus scale as the inverse sixth powder of the carbon–metal center distance. The carbon T1 measurements are summarized in Figure 7 for praseodymium acetate monohydrate where the CP-MASS methods were used[9-11] and the orientation de-

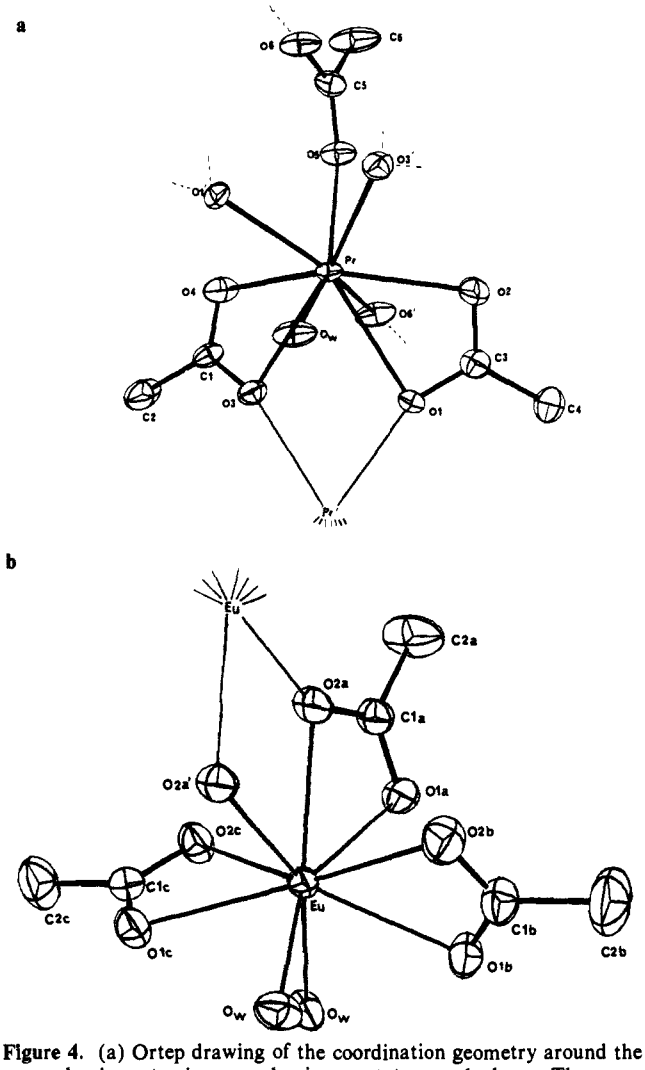

Figure 4. (a) Ortep drawing of the coordination geometry around the praseodymium aton in praseodymium acetate monohydrate. The water oxygen, Ow, is bonded to Pr(III) with an O···Pr distance of 2.541 (3) Å and is hydrogen bonded to O(6) and O(4) on inversion-related molecules. Dotted lines indicate bonds to neighboring molecules. The C(1) and C(3) acetate groups are bidentate and pseudomirror related. The C(5) acetate group is a bridging group bonded to a neighboring Pr(III) atom at ($1-x$, $0.5+y$, $0.5-z$). (b) Ortep drawing of the coordination geometry around the europium atom in europium acetate trihydrate. Two water molecules (water oxygens indicated by Ow) are directly bonded to Eu(III) with O···Eu distances of 2.397 and 2.393 Å. The third water oxygen, O3w, not shown in the diagram, is hydrogen bonded to one of these oxygens, to O2 (O3w···O2 = 2.724 Å) and to another O3w oxygen. All three acetate groups are bidentate. The C1a acetate group is unique in that it is the only one which is also coordinated to a neighboring europium center via an O2···Eu distance of 2.397 Å.

pendence of the relaxation rate in the powder is averaged by the rotor motion.[10,11] On this basis the slowly relaxed peaks are assigned to the methyl carbons and the rapidly relaxed peaks to the carboxyl carbons. The asymmetric unit in the crystal structure of praseodymium acetate (Figure 4a) suggests that three resonances of each type could be resolved; however, at 1.32 T we resolve only two (Figure 2A,B). The bonding patterns around the praseodymium atom shown in Figure 4a indicate that the two bidentate ligands are similar while the bridging acetate group is unique. The two bidentate acetate groups may become nearly magnetically equivalent because of the pseudo-mirror-symmetric chemical environment, apparently resulting in unresolved signals for C1 and C3 and for C2 and C4 with an intensity ratio of 2:1

(9) Torchia, D. A. *J. Magn. Reson.* **1978**, *30*, 613–616.

(10) Torchia, D. A.; Szabo, A. *J. Magn. Reson.* **1982**, *49*, 107–121.

(11) Naito, A.; Ganapathy, S.; McDowell, C. A. *J. Magn. Reson.* **1983**, *54*, 226–235.

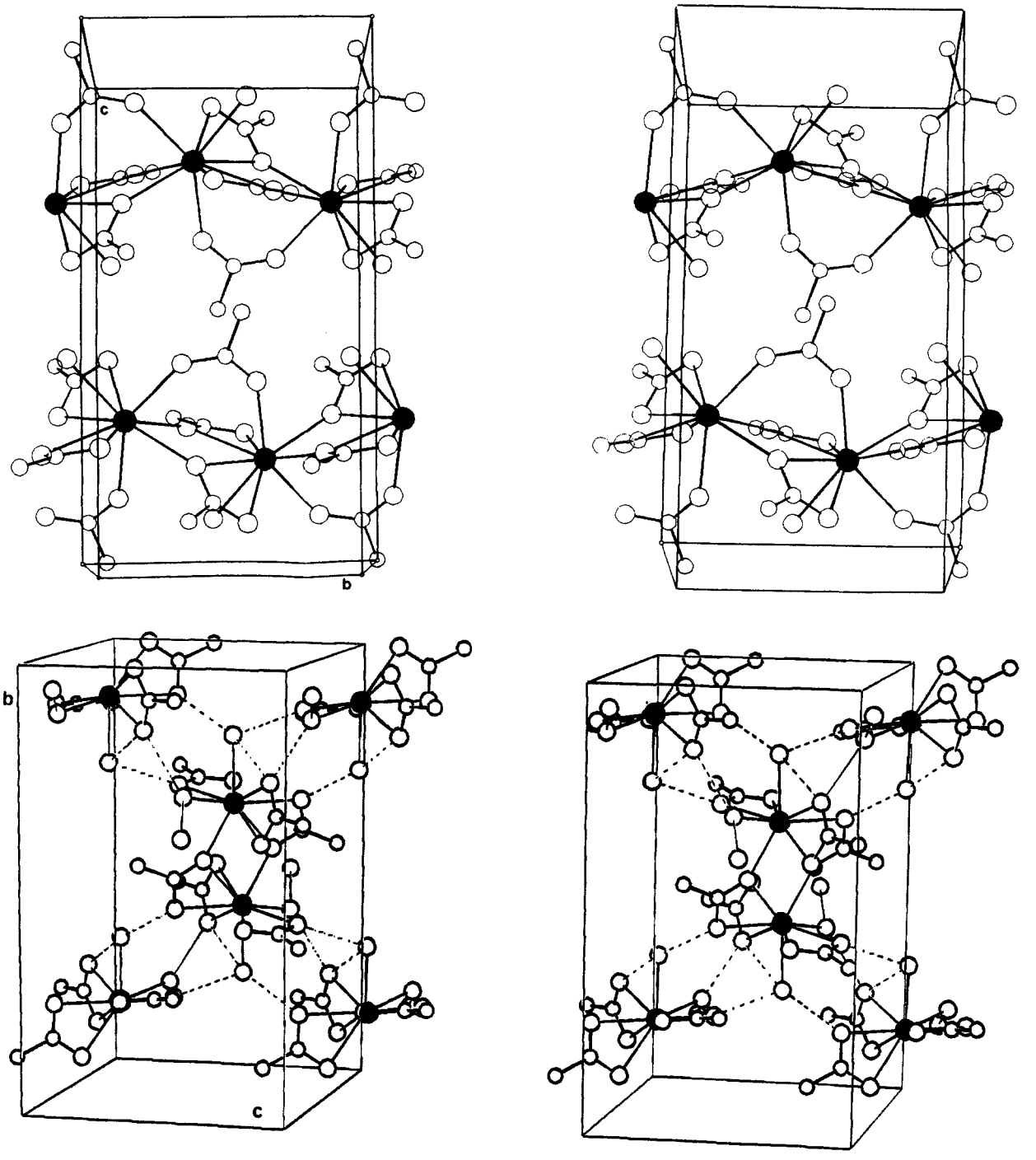

Figure 5. (a) An Ortep stereoscopic view along [100] of the unit cell of praseodymium acetate monohydrate. Hydrogen bonded chains of molecules extend along the *b*-screw axis. The bridging acetate groups are clearly visible in the center of the unit cells. The chemical environment is distinctly different from that of the bidentate acetate groups occurring within the molecular chains. Hydrogen bonds to water molecules are not shown, for clarity, but they do provide the mechanism for linking the two polymeric chains together in the crystal structure. Praseodymium atoms are shaded. (b) Ortep stereoscopic view, along [100] of the unit cell of europium(III) acetate trihydrate. Europium acetate chains parallel to the *c*-axis are formed via hydrogen bonds to water. The hydrogen bonds are shown by dotted lines. Strong Eu···O bonds between neighboring Eu and acetate groups, shown in the center of the unit cell, link the molecular chains together. These "intermolecular" bonds are actually shorter than the intramolecular Eu···O bond lengths. Europium atoms are shaded.

for these carbons compared to the respective unique bridging acetate carbons, C5 and C6.

The carboxyl and methyl carbons in europium acetate trihydrate were identified differently, although carbon selection using relaxation measurements would also be appropriate. Carbon selection using dipolar dephasing, introduced by Opella and Frey to differentiate between protonated and nonprotonated carbons in magic angle spinning experiments,[12] is not readily applicable to the identification of methyl groups,[13] although modifications to this scheme are available.[14] Since self decoupling of the C–H dipolar interaction does not take place for the europium acetate trihydrate, presumably because the proton T_1 is long compared with the reciprocal of the dipolar splitting, the total dipolar field at the carboxyl and methyl carbons are similar to those in the diagmagnetic case like calcium acetate. This view is supported experimentally by comparing spectra taken with and without

(12) Opella, S. J.; Frey, M. H. *J. Am. Chem. Soc.* **1979**, *101*, 5854–5856.

(13) Alemany, L. B.; Grant, D. M.; Alger, T. D.; Pugmire, R. J. *J. Am. Chem. Soc.* **1983**, *105*, 6697–6704.

(14) Murphy, P. D. *J. Magn. Reson.* **1985**, *62*, 303–308.

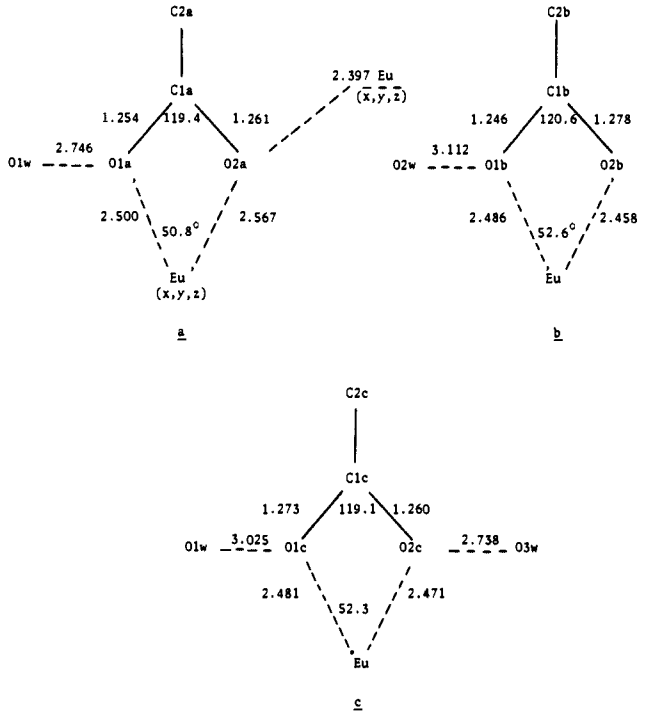

Figure 6. The coordination geometry for the three bidentate acetate groups in II. Group a also acts as a bridging group to europium on a molecule at $(-x, -y, -z)$.

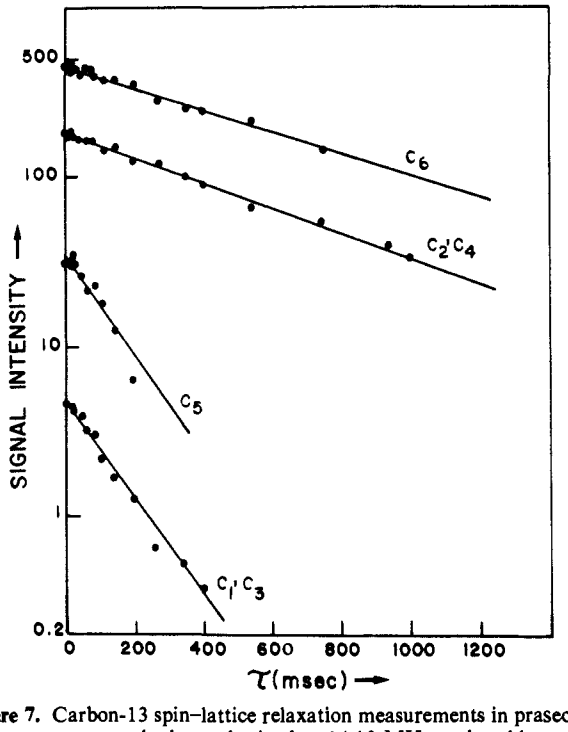

Figure 7. Carbon-13 spin–lattice relaxation measurements in praseodymium acetate monohydrate obtained at 14.19 MHz and ambient temperature by using a combination of CP-MASS and inversion recovery methods.[9,11] Least-squares analysis of the data yields the following T_1 values: C1, C3 = 155 ms; C5 = 125 ms; C2, C4 = 600 ms; C6 = 594 ms. These values support the assignments shown in Figure 2B.

proton decoupling shown for europium acetate trihydrate in Figure 8. Although MASS at 5 kHz averages the C–H dipolar interaction considerably, but not completely,[15] methyl carbons respond readily through increased broadening when the proton decoupling is removed as shown in Figure 8. There are three bidentate acetate groups as shown in Figure 4b. Only one of the groups

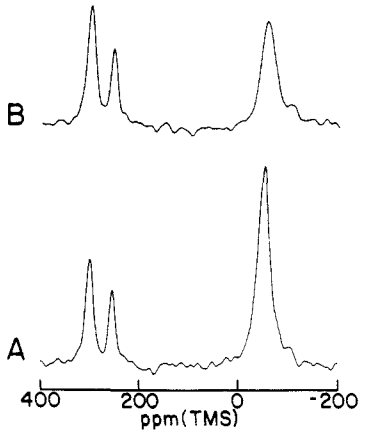

Figure 8. Carbon-13 CP-MASS spectra of europium(III) acetate trihydrate obtained at a rotor frequency of 4.8 kHz: (A) with 60 kHz proton decoupling; (B) without proton decoupling. Note the broadening of the resonance at −31 ppm on removal of the proton decoupling that leads to the identification of the methyl carbons in Figure 2D.

Table III. Carbon-13 Isotropic Chemical Shifts

compound	carbon atom[a]	chem shift, ppm from Me_4Si
lanthanum	carboxyl	+185.5
acetate[c]	methyl	+23.8
praseodymium	carboxyl: C1, C3	+211.0
acetate	C5	+115.4
monohydrate	methyl: C2, C4	+65.6
	C6	+28.8
europium	carboxyl: C1a	+274.4
acetate	C1b, C1c	+321.1
trihydrate	methyl: C1a, C2b, C2c	−30.8

[a] The carbon atoms are labeled according to the numbering scheme shown in the X-ray structure, Figure 4, and also correspond to the assignments indicated in Figure 2. [b] Positive values denote shifts to lower magnetic field strength. [c] Commerical sample, not recrystallized.

has an additional bond to a neighboring europium atom (through O2) so that C1a and C2a are geometrically close to two europium atoms, while the carbons on the other two acetate groups have only one europium atom within the same range. This geometry makes C1a and C2a quite different compared with C1c and C2c and C1b and C2b. This bonding configuration suggests that the paramagnetic shielding anisotropy for C1a should be greater than that for C1c. While this expectation cannot be discerned from the powder spectrum of Figure 1C, the larger anisotropy can be traced to the signal at 274 ppm in the CP-MASS spectrum (Figure 2C) because of the intense side band pattern, which maps the anisotropy,[16] for the carbon compared to that observed for the signal at 321 ppm. These considerations yield tentative assignments shown in Figure 2(C and D). As in praseodymium acetate monohydrate, C1b and C1c cannot be distinguished. Although the expected intensity ratio of 2:1 is also not observed precisely, the signal at 321 ppm is more intense than the one at 274 ppm (Figure 2D) suggesting that the intensity would be correct in the limit of very fast spinning, viz, $\nu_r \gg \Delta\sigma$. The methyl resonances are centered at −31 ppm and are not resolved at this field strength.

The isotropic chemical shifts for the lanthanide acetates studied here are summarized in Table III compared with the diamagnetic

(15) Andrew, E. R. *Prog. Nucl. Magn. Reson. Spectrosc.* **1971**, *8*, 1–39.

(16) Schaefer, J.; Stejskal, E. O. In *Topics in Carbon-13 NMR Spectroscopy*; Levy, G. C., Ed.; Wiley: New York, 1979; Vol. III, Chapter 4, 283–324.

(17) The commercial Alfa sample was labeled $Pr^{III}(O_2C_2H_3)\cdot 3H_2O$. We have demonstrated unambiguously using X-ray powder pattern analysis and single-crystal X-ray structure analysis that this sample is actually a monohydrate. Recrystallization from water gives a sample which has the same X-ray pwoder pattern as the unrecrystallized sample. The powder peak intensities and positions correlate unequivocally with single-crystal X-ray diffraction intensities from a single crystal of $Pr^{III}(O_2C_2H_3)\cdot H_2O$.

lanthanum acetate. It is clear that the paramagnetic shifts are substantial compared with the diamagnetic references, and as in solution applications of such compounds, the magnetic anisotropy may lead to significant changes in the positions compared with those expected from simple bonding pattern analogies.

Acknowledgment. This work was supported by the National Institutes of Health, GM-29428 and GM-34541. Helpful discussions with Professor Doyle Britton, University of Minnesota, are gratefully acknowledged.

Registry No. Pr(III) acetate·H_2O, 17829-83-3; Eu(III) acetate·$3H_2O$, 101953-41-7.

Supplementary Material Available: Positional and thermal parameters and their esd's (85 pages). Ordering information is given on any current masthead page.

Determining the Structure of a Glycopeptide–Ac_2-Lys-D-Ala-D-Ala Complex Using NMR Parameters and Molecular Modeling

S. W. Fesik,* T. J. O'Donnell, R. T. Gampe, Jr., and E. T. Olejniczak

Contribution from the Pharmaceutical Discovery Division, Abbott Laboratories, Abbott Park, Illinois 60064. *Received November 6, 1985*

Abstract: The interaction between ristocetin pseudo-aglycon and Ac_2-Lys-D-Ala-D-Ala, a model for the antibiotics' binding site of action, has been examined with NMR spectroscopy and molecular modeling. From a multispin analysis of the cross-peak volumes measured from a series of two-dimensional NOE experiments, many, accurate, proton–proton distances were obtained. These distance constraints along with vicinal spin–spin coupling constants and NH exchange rates were used to evaluate and modify computer-generated structures of the complex. Structures of the complex were energy minimized by applying different force fields, including one which contained an extra term, $K(r - r_0)^2$, used to constrain the interproton distances (r) in the computer-generated structure to the experimentally determined distances (r_0). Additional structures were generated from a short molecular dynamics trajectory. Two representative conformations were selected, minimized, and compared to the measured proton–proton distances. No single conformation was sufficient to explain all of the NMR data. The data were best explained by considering an average structure.

Vancomycin, a clinically useful glycopeptide antibiotic, has proven to be the drug of choice against methicillin resistant gram-positive bacteria.[1] Due to the recent increase of these types of infections,[2] vancomycin[3] and other members of this class of antibiotics (ristocetin,[4] avoparcin,[5] and teicoplanin[6]) have received a considerable amount of attention. It is believed that the glycopeptide antibiotics exert their antibiotic activity by binding to cell wall precursors terminating in D-alanyl-D-alanine.[7] In fact, the binding of di- and tripeptide models (Ac-D-Ala-D-Ala and Ac_2-Lys-D-Ala-D-Ala) of cell wall precursors correlates well with their antibiotic potencies.[8,9]

Using nuclear magnetic resonance spectroscopy, several investigators[10-13] have studied the structures of glycopeptide–peptide complexes. On the basis of the NMR data, the D-Ala-D-Ala binding site was found to be qualitatively similar in these studies; however, the proposed location of the Lys residue was found to be markedly different, depending on the antibiotic or solvent used in the study. Several other discrepancies exist in the structural models proposed for glycopeptide–peptide complexes. For example, Williams and co-workers[4,14] have postulated that an electrostatic interaction between the carboxylate anion of the peptide and the protonated amino terminus of ristocetin was important in the formation of the complex. Recently, however, the importance of this electrostatic interaction was questioned,[9] since a series of ristocetin analogues lacking a positively charged amino group all possessed antibacterial activity and were found to bind to Ac_2-Lys-D-Ala-D-Ala.

In addition to resolving the remaining ambiguities on the structure(s) of glycopeptide–peptide complexes, our studies are aimed at obtaining more detailed structures of the complexes than those previously reported. An important consideration in our work is how to use dynamic averaged NMR parameters to derive a structure or set of structures which represent the low-energy conformations about which most fluctuations occur. To obtain highly resolved structures, a large number of accurate distance constraints are required. Also, computational methods are needed to generate structures based on these distance constraints that are energetically reasonable and that can be quantitatively evaluated in terms of experimentally determined parameters.

In this report we have examined the interaction between ristocetin pseudo-aglycon and Ac_2-Lys-D-Ala-D-Ala in CD_3OD and CD_3OH. From a quantitative analysis of pure absorption two-dimensional NOE data sets, many accurate interproton distance constraints were obtained. These distance constraints along with spin–spin coupling constants and NH exchange rates were used to evaluate and modify computer graphical models of the complex generated from standard bond lengths and angles. Several ap-

(1) Griffith, R. S. *J. Antimicrob. Chemother.* **1984**, *14*, Suppl. D, 1.
(2) Crossley, K.; Loesch, D.; Landesman, B.; Mead, K.; Chern, M.; Strate, R. *J. Infect. Dis.* **1979**, *139*, 273.
(3) Farber, B. B. *Eur. J. Clin. Microbiol.* **1984**, *3*, 1.
(4) Williamson, M. P.; Williams, D. H.; Hammond, S. J. *Tetrahedron* **1984**, *40*, 569.
(5) (a) Ellestad, G. A.; Leese, R. A.; Morton, G. O.; Barbatschi, F.; Gore, W. E.; McGahren, W. J. *J. Am. Chem. Soc.* **1981**, *103*, 6522. (b) Fesik, S. W.; Armitage, I. M.; Ellestad, G. A.; McGahren, W. J. *Mol. Pharmacol.* **1984**, *25*, 275.
(6) (a) Borghi, A.; Coronelli, C.; Faniuolo, L.; Allievi, G.; Pallanza, R.; Gallo, G. G. *J. Antibiot.* **1984**, *37*, 615. (b) Hunt, A. H.; Molloy, R. M.; Occolowitz, J. L.; Marconi, G. G.; Debono, M. *J. Am. Chem. Soc.* **1984**, *106*, 4891. (c) Barna, J. C. J.; Williams, D. H.; Stone, D. J. M.; Leung, T. W. C.; Doddrell, D. M. *J. Am. Chem. Soc.* **1984**, *106*, 4895.
(7) Williams, D. H.; Rajananda, Vi.; Williamson, M. P.; Bojesen, G. In *Topics in Antibiotic Chemistry*; Sammes, P. G., Ed.; John Wiley & Sons, Inc.: New York, 1980; Vol. 5, p 119.
(8) Nieto, M.; Perkins, H. R. *Biochem. J.* **1971**, *124*, 845.
(9) Herrin, T. R.; Thomas, A. M.; Perun, T. J.; Mao, J. C.; Fesik, S. W. *J. Med. Chem.* **1985**, *28*, 1371.
(10) Convert, O.; Bongini, A.; Feeney, J. *J. Chem. Soc., Perkin Trans. 2* **1980**, 1262.
(11) Williams, D. H.; Williamson, M. P.; Butcher, D. W.; Hammond, S. J. *J. Am. Chem. Soc.* **1983**, *105*, 1332.
(12) Fesik, S. W.; Armitage, I. M.; Ellestad, G. A.; McGahren, W. J. *Mol. Pharmacol.* **1984**, *25*, 281.
(13) Williamson, M. P.; Williams, D. H. *J. Chem. Soc., Perkin Trans. 1* **1985**, 949.
(14) Barna, J. C. J.; Williams, D. H.; Williamson, M. P. *J. Chem. Soc., Chem. Commun.* **1985**, 254.

0002-7863/86/1508-3165$01.50/0